

Estimation and Mitigation of NCal Magnetic Coupling VIR-0753A-24

Florian Aubin, Eddy Dangelser, Benoit Mours,
Antoine Syx, Pierre Van Hove

IPHC-Strasbourg

April 23, 2024

Contents

1	Introduction	2
2	Magnetically induced strain	2
3	Origin of the magnetic field	4
4	Mitigation of the magnetic field	6
5	Conclusion	7

1 Introduction

The standard VIRGO Newtonian calibrators (NCals) are massive dipoles (fig. 1) which, when rotating at frequency f_{rot} , produce a sinusoidal gravitational force on the mirror **Test Mass (TM)** at twice the rotation frequency ($f_{2rot} = 2 * f_{rot}$). For the 04 observing run, two triplets of NCals were installed around the North End Mirror as shown in figure 2.

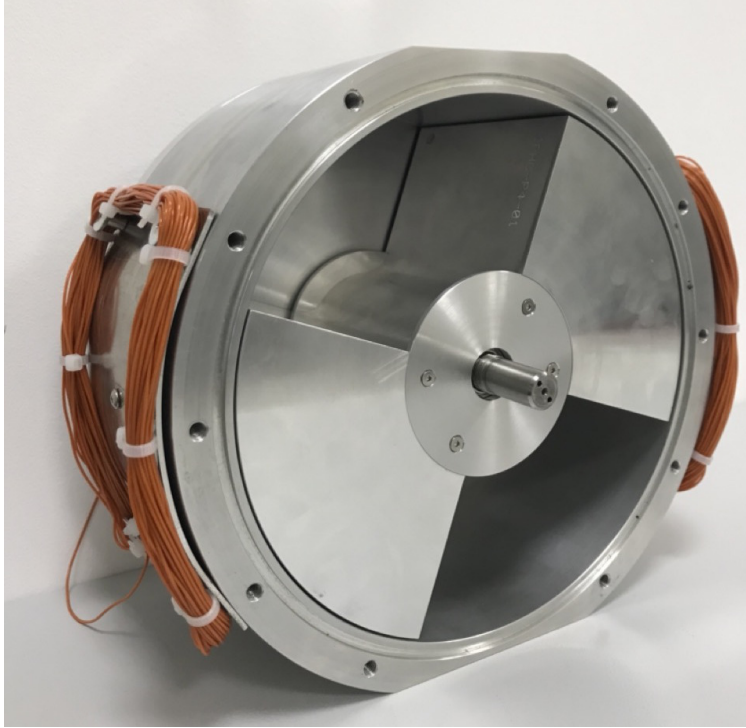


Figure 1: Side view of one opened NCal with a two-sector aluminum rotor. Two coils (orange wires) have been attached on each side of the NCal to study the magnetic fields produced by the NCal.

In the aim to reach a subpercent calibration precision of the VIRGO detector, any possible parasitic coupling needs to be estimated and mitigated. In this note, we focus on the parasitic magnetic field produced by the NCal. This magnetic field was first observed on April 7th 2023 by the VIRGO environmental group¹. Using the environmental magnetic sensors (ENV_NEB_MAG_V) which was temporarily placed at the base of the tower close to the North NCal setup, the amplitude of the observed magnetic field at twice the rotor frequency ranged from $B_{MAG_V} = 0.001 \text{ nT}$ to $B_{MAG_V} = 0.1 \text{ nT}$ as can be deduced from figure 3.

2 Magnetically induced strain

Magnetic field effect on the **TM** has been simulated in [1] and transfer function from magnetic field to mirror oscillation has been experimentally measured through the use of large electro-magnet (VIR-0688A-23). Using the upper value of the experimental transfer function ($\lesssim 10^{-10} \text{ m/T}$ for $\nu > 30 \text{ Hz}$), the parasitic signal induced by the magnetic field of the NCal on the mirror can be estimated as $h_B(NCal) \lesssim 10^{-20} \text{ m}$ to be compared to the corresponding gravitational signal of about $h_g(NCal)(f_{2rot} = 30 \text{ Hz}) \sim 10^{-18} \text{ m}$.

¹Estimation from the VIRGO logbook (<https://logbook.virgo-gw.eu/virgo/?r=59699>)

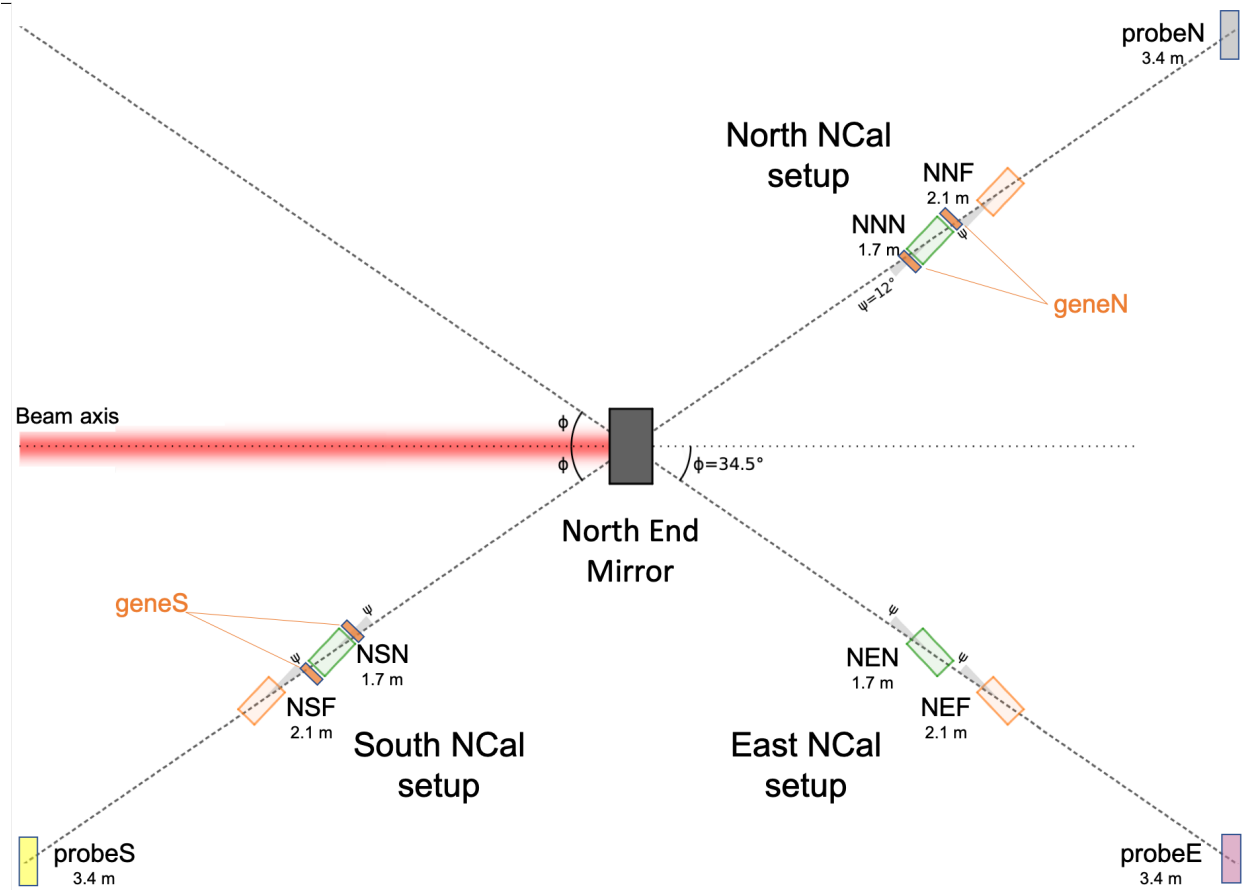


Figure 2: Top view of the NCal setup in **North End Building (NEB)** with two triplets of rotors. Each rotor is identified by three letters: the end mirror (N for North), the NCal position relative to the mirror (N for North, S for South and E for East), and the triplet identifier (N for Near and F for Far). The rotors are twisted by an angle $\Psi = 12^\circ$ with respect to the setup direction. Two pairs of generating solenoids (geneN and geneS) are placed around NNN and NSN rotors respectively. Three probe solenoids (probeE, probeN and probeS) are placed on each setup direction, at a distance to the corresponding near rotor equaling the near rotor to mirror distance.

From this first estimation, the maximal relative uncertainty induced by magnetism is around 1%, small but not negligible compared to our sub-percent precision target.

To produce an independent estimation of this uncertainty, that takes account of the setup geometry, we equipped the NCal system with coils to generate and measure magnetic field (see fig. 2). Two generating coils (geneN and geneS) each consist of a pair of wire loops placed on each side of the North and South corresponding rotor (fig.1). Each loop is a rectangle of $11 * 15 \text{ cm}^2$ with 50 turns of wire and can be powered in DC or at various frequencies to generate a sinusoidal dipole magnetic field. Three probe coils (probeN, probeS and probeE) are used to measure magnetic field variations. They consist in a solenoid of about 760 turns with an internal radius of $R_{int} = 106 \text{ mm}$, an external radius of $R_{ext} = 116 \text{ mm}$ and a length of 90 mm . On each setup direction (North, South and East), the probes are placed at 1.7 m from the corresponding rotor which is itself at 1.7 m from the mirror. By symmetry, for each setup, the field measured by the probe and produced by the Near NCal or gene coil must equal the produced field on the **TM**. For the Far NCal, as the coil-rotor distance is shorter than the rotor-mirror distance, the measured magnetic field must be corrected

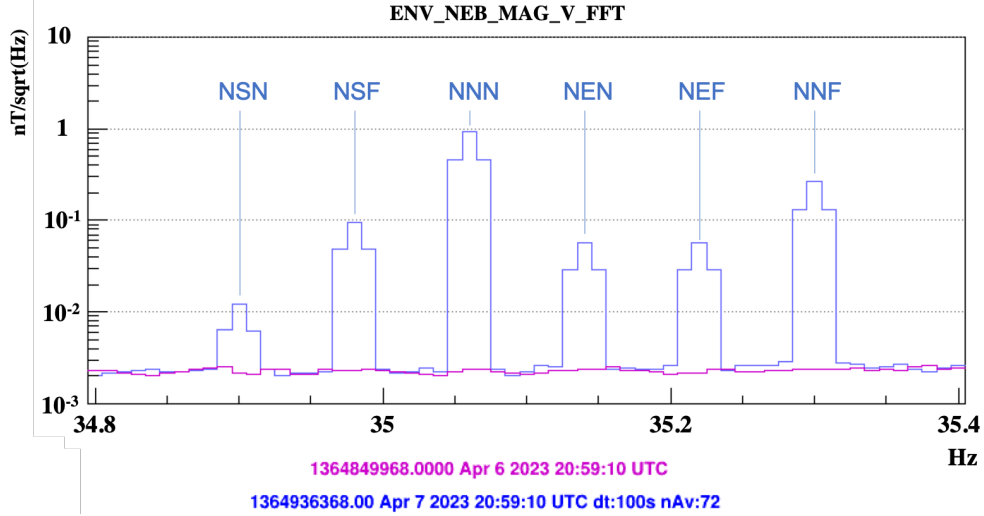


Figure 3: Measure of magnetic field with FFT of 100s using ENV_NEB_MAGV sensor placed at the base of the NEB tower. Pink (resp. blue) curve corresponds to magnetic field with stopped (resp. rotating) rotors. The rotor names above the peaks correspond to twice the frequency of the corresponding rotor. The values of the peaks range from 0.001 to 0.1 nT.

by a "mirror to probe" field correction of at least 4.2^2 .

Using this configuration, with the VIRGO interferometer locked, we measured from December 12 2023 at 23h00 UTC to December 13 2023 at 6h00 the $h(f)$ signal and the magnetic field produced by the NCal and by the generating loops (see table 1). A simple cross multiplication, taking into account the "mirror to probe" field correction, then yields the proportion of magnetic to total strain (h_B/h) produced by the rotor (see table 1). Note that, for these measurements, all the rotors were in aluminium and two of them (NNF and NSF)³ were shielded with a MCL61 foil from YSHILD®⁴.

The results confirm and consolidate the first estimation from the transfer function. For the Near unshielded rotors at least, this magnetic coupling induces an uncertainty of the order of 0.5%. In order to have an absolute calibration below the percent level, this situation requires improvement.

3 Origin of the magnetic field

To mitigate the magnetic field effect, it is important to understand its origin. Three possible sources were experimentally tested: the electric motor of the NCal, residual magnetic field inside the aluminium material of the rotor and eddy currents produced inside the aluminium when the rotor is rotating.

To differentiate these possibilities, we first made several tests by changing the rotor of the tested NCal with a three-sector aluminium rotor, a two-sector copper rotor (copper is diamagnetic while aluminium is paramagnetic) and a two-sector PVC rotor (see fig. 4). These tests were performed in our Strasbourg laboratory with a setup similar to the Virgo setup in term of angle but with the probe coil placed at a distance of only 40cm from the NCal to increase the sensitivity of the measurement.

²If we use the conservative assumption that the rotor magnetic field decrease with the cube of the distance (dipole field) then, with a coil-rotor distance of 1.3 m and rotor-mirror distance of 2.1 m , the overestimation is of the order of $(2.1/1.3)^3 \sim 4.2$.

³<https://logbook.virgo-gw.eu/virgo/?r=62639>

⁴https://expercem.com/product.php?id_product=350

source	$f(Hz)$	B(a.u.)	snr(B)	$h(f) \times 10^{23}$	snr($h(f)$)	$h_B(NCal)/h(NCal)(\%)$
geneN	40.82	116.4	329	1.3	11	
NNF	40.98	3.1	9	56.1	495	≤ 0.01
NSF	41.04	37.7	106	54.8	485	≤ 0.2
NNN	41.16	34.6	98	130.4	1153	0.3
NSN	41.22	60.7	172	124.9	1104	0.6
geneS	41.28	86.3	244	1.1	10	

Table 1: Magnetic field and strain produced by the generating coil and NCal rotors. " $f(Hz)$ " is the frequency at which the signal is measured. "B(a.u.)" is the signal observed on the probe from the corresponding setup direction (probeN for North gene or North NCal, probeS for South gene or South NCal). " $h(f)$ " is the strain signal observed in virgo and last column correspond to the ratio of magnetically induced NCal strain to the total NCal strain.

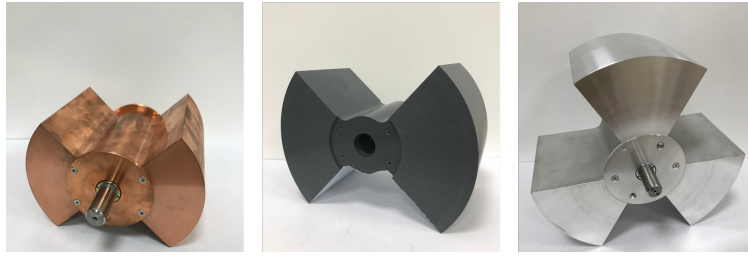


Figure 4: Image of the copper (left), PVC (middle) and three-sector aluminium (right) rotors tested in place of the nominal aluminium.

When using the three-sector aluminium rotor, the induced magnetic field does not anymore appear at twice but at three time the rotation frequency (see fig. 5). This excludes the motor and points to the rotor itself as a source of magnetic field. For the test with the copper rotor the observed magnetic field was at the same order of magnitude than for the aluminium rotor. Finally, the test with the PVC rotor, showed a magnetic field reduction of more than two order of magnitude with respect to the aluminium rotor. These results are summarized in table 2.

Twist ($^\circ$)	B(Al)(a.u.)	B(PVC) (a.u.)	B(Cu) (a.u.)	B(Al)/B(PVC)	B(Al)/B(Cu)
90°	1.26×10^{-4}	8.79×10^{-7}	5.16×10^{-5}	143	2.4
12°	3.05×10^{-4}	17.7×10^{-7}	24.2×10^{-5}	172	1.3
-90°	1.43×10^{-4}	10.4×10^{-7}	10.4×10^{-5}	139	1.4
-168°	4.71×10^{-4}	21.0×10^{-7}	21.5×10^{-5}	224	2.2

Table 2: Magnetic field measured with Al, PVC and Copper rotor at twice the rotation frequency. Test were performed in our Strasbourg laboratory with a distance between the NCal and the probe of $40cm$. The first column is the twist angle Ψ of the rotor with respect to the setup direction as defined in figure 2. The last two columns give the ratio of Al to PVC and AL to Cu magnetic field.

These three tests point to eddy currents as the main cause of the magnetic field. To confirm this, using again the two-sector aluminium rotor, we tested how the amplitude of $B_{rot}(f_{2rot})$ changes when we apply a constant magnetic field (B_{env}) in the rotor region.

To generate B_{env} , we use the pair of "Generating Coils" (gene) placed on each side of the rotor box (fig. 1). A rough theoretical estimation shows that with a current $I = 1A$, the magnetic field produced by these coil at the center of the box is about $B_{env}(1) \approx 91\mu T$ ⁵.

⁵This can be compared to Strasbourg Earth magnetic field $B_{Earth} \approx 48\mu T$ (from <https://www.ngdc.noaa.gov/geomag/calculators/magcalc.shtml>)

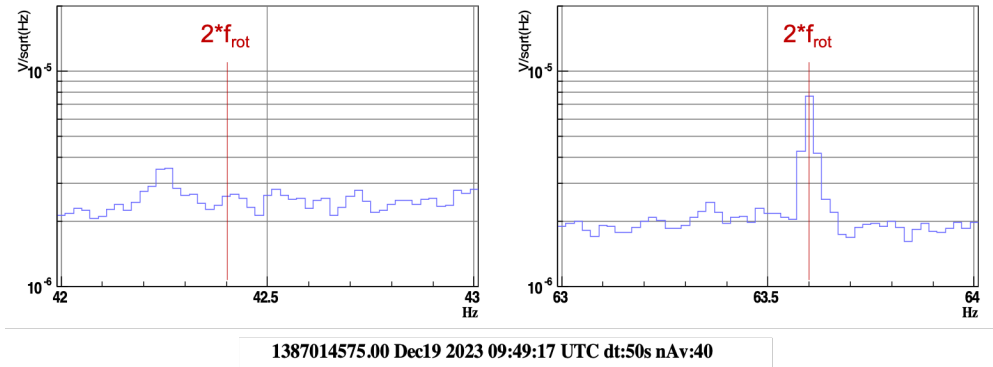


Figure 5: Magnetic signal generated by a three-sector rotor. Left: zoom around twice the rotor frequency (21.2 Hz). Right: zoom around three times the rotor frequency.

An experimental value of the magnetic field inside the rotor housing (B_{env}) is obtained with a smartphone and the "Phyphox" application.⁶ To experimentally measure the amplitude of the magnetic field produced by the rotor (B_{rot}), we use one of our probe coils and compute a Fast Fourier Transform (FFT) with a length of 10s of the differential voltage signal at the extremities of the wireloop.

The values of these two measurements are presented in table 3 and in figure 6. One clearly sees the strong correlation between $B_{env_{\perp}}$ and B_{rot} when the current is changed. This nicely confirm that the main source of B_{rot} are eddy currents.

$I(A)$	$B_{env_x}(\mu T)$	$B_{env_y}(\mu T)$	$B_{env_z}(\mu T)$	$B_{rot}(f_{2rot})(a.u.)$
-1.0	-112.8	-31.6	-2.4	0.2012
-0.8	-88.3	-32.5	-2.8	0.1608
-0.4	-39.1	-34.3	-3.7	0.0875
-0.2	-14.6	-35.2	-4.1	0.0671
0.0	9.7	-36.2	-4.5	0.0725
0.2	34.5	-37.1	-4.9	0.1002
0.4	59.1	-38.0	-5.4	0.1371
0.8	108.2	-39.8	-6.2	0.2187
1.0	132.8	-40.8	-6.6	0.2616

Table 3: Estimation of B_{env} and B_{rot} for current ranging from $-1A$ to $1A$. X-axis correspond to the gene coil axis, Y-axis is vertical and Z-axis is parallel to the rotor axis.

4 Mitigation of the magnetic field

To mitigate the produced magnetic field and its effect on the TM, we tested two solutions: a minimal shielding with a MCL61 foil wrapping the NCal and replacing aluminium rotor with a resistive and precisely machinable material.

The wrapping method has two effect: it contains the sinusoidal magnetic field within the wrapped volume and it shields the rotor volume from the external constant magnetic field (e.g. Earth magnetic field). With the wrapping method used, the observed diminution of magnetic field was about a factor of 3. This was a good but relatively deceptive results considering the supposed combined action and we will investigate better shielding in the future. In this process, we also observed that the axis of the rotors are themselves magnetic

⁶<https://phyphox.org/>

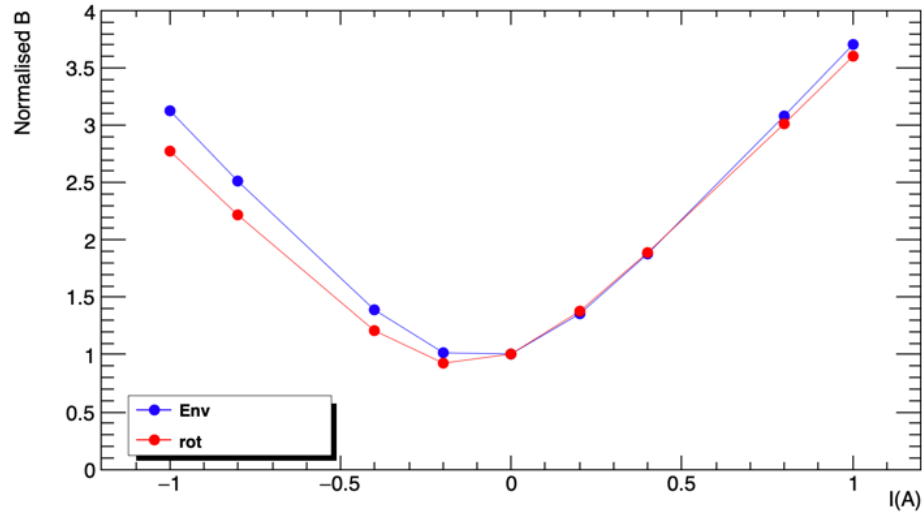


Figure 6: Normalised magnetic fields as a function of PC current. In red, the field produced by the rotor. In blue, the environmental magnetic field (due to Earth + PC) transverse to the rotor axis ($B_{env\perp}$). Both are normalised to their value at $I = 0A$.

and produce a magnetic field inside the rotor box mitigating the shielding effect of the wrapping. Future tests of shielding improvement will also be combined with the replacement of these axis with non-magnetic stainless-steel.

The resistive material solution was tested by replacing the aluminium rotor by Polyvinyl Chloride (PVC) rotor. PVC has an electric resistivity about 10^{21} times higher than aluminium and, as eddy current are proportional to the conductance of the material, the produced magnetic field by this current should become negligible. Measuring the effect in our Strasbourg laboratory with one of our probe coils, we found that the magnetic signal is not null but reduced by at least two order of magnitude (see table 2). This solution is easy to implement and provides very good magnetic field attenuation but it has two drawbacks. As PVC is twice lighter than aluminium, the expected Newtonian signal used for VIRGO calibration is twice smaller and as PVC is more elastic than aluminium, a larger corresponding systematic effect must be accounted for.

5 Conclusion

Due to eddy current in the aluminium NCal rotating in a constant magnetic field, the two-sector NCal produce oscillating magnetic field at twice the rotating frequency with an amplitude ranging from 0.001 to 0.1 nT near the NEB tower. This magnetic field in turns produces a parasitic oscillation of the mirror which we estimated to be of the order of 0.5% of the total NCal induced signal for the Near position.

Wrapping the NCal with a shielding foil (MCL61 from YSHILD®) reduces by a factor of three the produced magnetic field. This solution was implemented at the start of 04 for the FAR NCal. With these shielding, the magnetic parasitic coupling of the FAR NCal was estimated to less than 0.2% of the total signal.

Replacing the aluminium rotor by PVC rotor reduces the produced magnetic field by at least two order of magnitude. As the expected gravitational signal is decreased by a factor of 2 due to the lower mass of the PVC rotor, the relative magnetic parasitic coupling is reduced by a factor of 50. This solution was implemented at the start of 04 for the NEAR NCal leading to a corresponding relative uncertainty of less than 0.012%.

For the start of O4b, the FAR aluminium rotor were also replaced by PVC rotors. With this setup, the magnetic

coupling is now negligible with respect to other uncertainties.

For future improvement, it is possible that PVC will have to be replaced. First because of its lower weight and corresponding gravitational signal and second because of its larger elasticity that increase the corresponding uncertainty and decrease the highest possible rotation frequency. Other materials such as polyether ether ketone (PEEK) are investigated and the shielding solution also needs to be considered. For this later, using non-magnetic stainless-steel axis will be a first step as it will lower the constant magnetic field inside the wrapping shielding foil.

References

- [1] A. Cirone *et al.*, “Magnetic coupling to the advanced Virgo payloads and its impact on the low frequency sensitivity,” *Review of Scientific Instruments*, vol. 89, no. 11, p. 114501, Nov. 2018.